Article

Binding of Serotonin to the Human Serotonin Transporter. Molecular Modeling and Experimental Validation

Leyla Celik, Steffen Sinning, Kasper Severinsen, Carsten G. Hansen, Maria S. Mller, Mikael Bols, Ove Wiborg, and Birgit Schitt

J. Am. Chem. Soc., **2008**, 130 (12), 3853-3865 • DOI: 10.1021/ja076403h

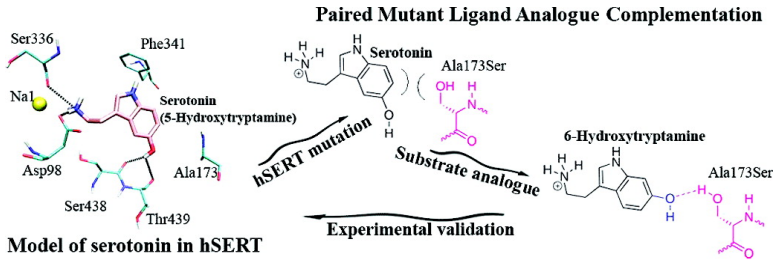

More About This Article

Additional resources and features associated with this article are available within the HTML version:

- Supporting Information
- Links to the 2 articles that cite this article, as of the time of this article download
- Access to high resolution figures
- Links to articles and content related to this article
- Copyright permission to reproduce figures and/or text from this article

View the Full Text HTML

J|A|C|S
ARTICLES
Published on Web 03/04/2008

Binding of Serotonin to the Human Serotonin Transporter. Molecular Modeling and Experimental Validation

Leyla Celik,[§] Steffen Sinning,[‡] Kasper Severinsen,[‡] Carsten G. Hansen,[‡] Maria S. Møller,[†] Mikael Bols,[†] Ove Wiborg,*[,‡] and Birgit Schiøtt*[,§]

The iNANO and inSPIN Centers, the Department of Chemistry, University of Aarhus, Aarhus, Denmark, and the Laboratory of Molecular Neurobiology, Centre for Psychiatric Research, Aarhus University Hospital, Risskov, Denmark

Received August 25, 2007; E-mail: owiborg@post.tele.dk; birgit@chem.au.dk

Abstract: Molecular modeling and structure−activity relationship studies were performed to propose a model for binding of the neurotransmitter serotonin (5-HT) to the human serotonin transporter (hSERT). Homology models were constructed using the crystal structure of a bacterial homologue, the leucine transporter from *Aquifex aeolicus*, as the template and three slightly different sequence alignments. Induced fit docking of 5-HT into hSERT homology models resulted in two different binding modes. Both show a salt bridge between Asp98 and the charged primary amine of 5-HT, and both have the 5-HT C6 position of the indole ring pointing toward Ala173. The difference between the two orientations of 5-HT is an enantiofacial discrimination of the indole ring, resulting in the 5-hydroxyl group of 5-HT being vicinal to either Ser438/Thr439 or Ala169/Ile172/Ala173. To assess the binding experimentally, binding affinities for 5-HT and 17 analogues toward wild type and 13 single point mutants of hSERT were measured using an approach termed paired mutant−ligand analogue complementation (PaMLAC). The proposed ligand−protein interaction was systematically examined by disrupting it through site-directed mutagenesis and re-establishing another interaction *via* a ligand analogue matching the mutated residue, thereby minimizing the risk of identifying indirect effects. The interactions between Asp98 and the primary amine of 5-HT and the interaction between the C6-position of 5-HT and hSERT position 173 was confirmed using PaMLAC. The measured binding affinities of various mutants and 5-HT analogues allowed for a distinction between the two proposed binding modes of 5-HT and biochemically support the model for 5-HT binding in hSERT where the 5-hydroxyl group is in close proximity to Thr439.

1. Introduction

The serotonin transporter (SERT), responsible for reuptake of serotonin (5-hydroxytryptamine, 5-HT) into the presynaptic neuron, is the primary target for treatment of anxiety and depression[1−3] and belongs to the monoamine transporter subfamily of neurotransmitter sodium symporters (NSSs).[4] Depression can be treated by tricyclic antidepressants (TCAs), as imipramine and amitriptyline, or by selective serotonin reuptake inhibitors (SSRIs) such as citalopram, paroxetine, fluoxetine, sertraline, and fluvoxamine.[5,6] SERT is also a target for drugs of abuse, e.g., 3,4-methylenedioxymethamphetamine (ecstasy)[7] and cocaine.[8]

The 3D structure of SERT is so far unknown.[9] However, from hydropathy plots it has been predicted to consist of 12 transmembrane (TM) α-helices with the N- and C-termini located intracellularly.[6] Experimental data[10,11] have confirmed the predicted topology. The first crystal structure of a bacterial homologue of the NSS proteins, the *Aquifex aeolicus* leucine transporter, $LeuT_{Aa}$, was published in 2005[12] and new structures of $LeuT_{Aa}$ with bound TCAs, have recently appeared.[13,14] The structures show a novel fold for a membrane bound transporter with 12 TM helices where TM1−5 and TM6−10 are related by a pseudo 2-fold axis having TM1 and TM6 unwound in the middle to make up the binding site along with TM3 and TM8, both of which are kinked around the binding site.[12] The amphiphilic binding site contains a substrate leucine residue along with two sodium ions, one of which is directly coordinated

[§] *i*NANO and *in*SPIN Centers, Department of Chemistry.
[‡] Centre for Psychiatric Research.
[†] Department of Chemistry.

(1) Fuller, R. W.; Wong, D. T. *Ann. N. Y. Acad. Sci.* **1990**, *600*, 68−80.
(2) Hahn, M. K.; Blakely, R. D. *Pharmacogen. J.* **2002**, *2*, 217−235.
(3) Owens, M. J.; Nemeroff, C. B. *Clin. Chem.* **1994**, *40*, 288−295.
(4) Nelson, N. *J. Neurochem.* **1998**, *71*, 1785−1803.
(5) Oh, S. J.; Ha, H. J.; Chi, D. Y.; Lee, H. K. *Curr. Med. Chem.* **2001**, *8*, 999−1034.
(6) Ramamoorthy, S.; Bauman, A. L.; Moore, K. R.; Han, H.; Yang-Feng, T.; Chang, A. S.; Ganapathy, V.; Blakely, R. D. *Proc. Natl. Acad. Sci. U.S.A.* **1993**, *90*, 2542−2546.
(7) Trigo, J. M.; Renoir, T.; Lanfumey, L.; Hamon, M.; Lesch, K.; Robledo, P.; Maldonado, R. *Biol. Psych.* **2007**, *62*, 669−679.
(8) Sora, I.; Hall, F. S.; Andrews, A. M.; Itokawa, M.; Li, X.; Wei, H.; Wichems, C.; Lesch, K.; Murphy, D. L.; Uhl, G. R. *Proc. Natl. Acad. Sci. U.S.A.* **2001**, *98*, 5300−5305.
(9) Rudnick, R. *J. Membr. Biol.* **2006**, *213*, 101−110.
(10) Androutsellis-Theotokis, A.; Rudnick, G. *J. Neurosci.* **2002**, *22*, 8370−8378.
(11) Chen, J.; Liu-Chen, S.; Rudnick, G. *J. Biol. Chem.* **1998**, *273*, 12675−12681.
(12) Yamashita, A.; Singh, S. K.; Kawate, T.; Jin, Y.; Gouaux, E. *Nature* **2005**, *437*, 215−223.
(13) Singh, S. K.; Yamashita, A.; Gouaux, E. *Nature* **2007**, *448*, 952−956.
(14) Zhou, Z.; Zhen, J.; Karpowich, N. K.; Goetz, R. M.; Law, C. J.; Reith, M. E. A.; Wang, D.-N. *Science* **2007**, *317*, 1390−1393.

to the substrate. It has been suggested that this sodium ion (Na1) is cotransported, while the second ion (Na2) may play a structural role.[12] Toward the extracellular side of the transporter the binding site is only closed by an aromatic lid (residues Tyr108 and Phe252) and a salt bridge (residues Arg30 and Asp404). The $LeuT_{Aa}$ structures with bound TCAs have these located outside the salt bridge. On the basis of the occluded conformation of the $LeuT_{Aa}$ structure, the facilitated transport is suggested to consist of at least three different conformations of the protein[12] to follow the *alternate access* theory for transporters.[15] The high-resolution 3D structure of $LeuT_{Aa}$ with bound substrate leucine has paved an avenue toward the construction of homology models of the neurotransmitter transporters and further medicinal chemistry approaches.[9]

The observation by Chotia and Lesk[16] that 3D structure is a more conserved property during evolution than is the sequence of proteins belonging to the same family, supports the use of $LeuT_{Aa}$ as a template for homology modeling of the human NSSs despite low overall sequence identity.[9,12] As pointed out by Yamashita et al.[12] an interesting difference between $LeuT_{Aa}$ and monoamine transporters is the substitution of a glycine residue (Gly24) in the $LeuT_{Aa}$ binding site to an acidic residue in the monoamine transporters. They propose that the carboxylate in the substrate leucine in $LeuT_{Aa}$ is replaced by a carboxylate functionality in the NSSs at the position corresponding to Gly24 in $LeuT_{Aa}$; for SERT this is Asp98, hereby complementing the difference in substrate between $LeuT_{Aa}$ (an amino acid) and SERT (an amine). This is a classic example of the deletion model as proposed for the evolution of selective receptors.[17] A further indication that the $LeuT_{Aa}$ structure is a good template for modeling of NSS proteins is found in an elegant study by Dodd and Christie.[18] On the basis of the $LeuT_{Aa}$ structure and sequence alignments of the creatine and γ-aminobutyric acid (GABA) transporters, both of which also belong to the NSS family, they were able to change the substrate specificity of the creatine transporter by mutating a few residues in the putative binding pocket of the creatine transporter to their respective counterparts of the GABA transporter thereby switching it to a transporter selective for GABA.[18] This suggests that substrate specificity of the transporters is defined by the actual amino acids lining the central binding cavity and that this central cavity is common to the members of the NSS family.

Site-directed mutagenesis has previously been employed in numerous studies in an attempt to identify residues lining the primary ligand binding site in SERT, as well as in the dopamine transporter (DAT) and the norepinephrine transporter (NET). Some have been successful, but after the publication of the structure of $LeuT_{Aa}$[12] a significant proportion of the residues suggested to interact directly with a ligand are more likely to influence ligand binding in an indirect manner. However, with the mutagenesis studies and the $LeuT_{Aa}$ structure at hand it seems very evident that Asp98[19] and Ala169[20] interact with 5-HT, and in addition Ile172[20,21] is likely to interact with some inhibitors.

In order to eliminate the possibility of observed trends in measured binding affinities being due to allosteric effects, we decided to explore the binding of 5-HT in human SERT (hSERT) in a systematic and quantitative manner by using molecular modeling to rationally design pairs of protein mutants and substrate analogues. A structural change of a ligand that affects its binding affinity can be reversed by a specific, complementing, mutation of the transporter. We call this experimental paradigm "paired mutant−ligand analogue complementation" (PaMLAC) and find that it alleviates several of the reservations associated with mutational analysis of ligand binding by supplying a second layer of experimental evidence and additionally firmly establish which part of the ligand interacts with which residue in the transporter. The PaMLAC paradigm relies heavily on the availability of a wide ensemble of ligand analogues and protein mutants but also very much on reliable structural molecular models to provide testable predictions of protein−ligand interactions. The idea of coupling protein mutational studies with binding affinities for substrate analogues has previously been attempted by Strader et al. in the 1980s[22,23] in a study of the β-adrenergic receptor. However, they did not have a 3D model from which rational predictions could be made and therefore did not explore the interactions systematically. To the best of our knowledge, resolution of ligand−protein interactions in hSERT to such a degree of detail has been very scarce in the literature, a study from Barker et al. being the most comprehensive so far.[19]

To predict the binding of substrate 5-HT to hSERT, we first have to build a homology model of hSERT based on the template $LeuT_{Aa}$ structure and then predict the structure and orientation of the substrate in the binding cavity by using molecular docking. This approach possesses several computational challenges as are evident from the preliminary homology models of NSS proteins that have appeared in the literature.[24−30] In these studies a ligand was modeled in the binding site of the selected transporters by a manual placement since the use of automated docking procedures for this purpose so far has failed. A comprehensive examination of a model describing the binding orientation of 5-HT in the binding site of hSERT, including biochemical validation, has not yet appeared in the literature.

Homology modeling of membrane proteins is, compared to homology modeling of globular water soluble proteins, a new research area, as the number of templates is rather limited. However, it has recently been shown that homology modeling methods are as applicable to membrane proteins as they are to water soluble proteins,[31] meaning that good quality homology

(15) Jardetzky, O. *Nature* **1966**, *211*, 969−970.
(16) Chotia, C.; Lesk, A. M. *EMBO J.* **1986**, *5*, 823−826.
(17) Topiol, S. *Trends Biochem. Sci.* **1987**, *12*, 419−421.
(18) Dodd, J. R.; Christie, D. L. *J. Biol. Chem.* **2007**, *282*, 15528−15533.
(19) Barker, E. L.; Moore, K. R.; Rakhshan, F.; Blakely, R. D. *J. Neurosci.* **1999**, *19*, 4705−4717.
(20) Larsen, M. B.; Elfving, B.; Wiborg, O. *J. Biol. Chem.* **2004**, *279*, 44147−44156.
(21) Henry, L. K.; DeFelice, L. J.; Blakely, R. D. *Neuron* **2006**, *49*, 791−796.
(22) Strader, C. D.; Sigal, I. S.; Candelore, M. R.; Rands, E.; Hill, W. S.; Dixon, R. A. F. *J. Biol. Chem.* **1988**, *263*, 10267−10271.
(23) Strader, C. D.; Candelore, M. R.; Hill, W. S.; Sigal, I. S.; Dixon, R. A. F. *J. Biol. Chem.* **1989**, *264*, 13572−13578.
(24) Zomot, E.; Bendahan, A.; Quick, M.; Zhao, Y.; Javitch, J.; Kanner, B. *Nature* **2007**, *449*, 726−730.
(25) Beuming, T.; Shi, L.; Javitch, J. A.; Weinstein, H. *Mol. Phamacol.* **2006**, *70*, 1630−1642.
(26) Jørgensen, A. M.; Tagmose, L.; Jørgensen, A. M. M.; Topiol, S.; Sabio, M.; Gundertofte, K.; Bøgesø, K. P.; Peters, G. H. *ChemMedChem* **2007**, *2*, 815−826.
(27) Paczkowski, F. A.; Sharpe, I. A.; Dutertre, S.; Lewis, R. J. *J. Biol. Chem.* **2007**, *282*, 17837−17844.
(28) Ravna, A. W.; Sylte, I.; Kristiansen, K.; Dahl, S. G. *Bioorg. Med. Chem.* **2006**, *14*, 666−675.
(29) Sen, N.; Shi, L.; Beuming, T.; Weinstein, H.; Javitch, J. A. *Neuropharm.* **2005**, *49*, 780−790.
(30) Forrest, L. R.; Tavoulari, S.; Zhang, Y.-W.; Rudnick, G.; Honig, B. *Proc. Natl. Acad. Sci. U.S.A.* **2007**, *104*, 12761−12766.
(31) Forrest, L. R.; Tang, C. L.; Honig, B. *Biophys. J.* **2006**, *91*, 508−517.

models can be expected if the sequence identity in the TM regions is approximately 30% or above and the template structure is of high resolution (meaning below 2.0 Å in the TM regions). If these criteria are fulfilled, the homology models generated are expected to have a Cα-RMSD (root-mean-square deviation) of ~2 Å from the native structure of the protein.[31] Specifically, it was found that the TM regions of homology models of membrane proteins are modeled with higher accuracy than the domains of the protein not embedded in the membrane, possibly due to the fact that the surrounding lipids in the membrane restrict the flexibility of the TM regions.[31] In our case these two prerequisites are fulfilled as the structure of $LeuT_{Aa}$ was solved at a resolution of 1.65 Å, and the sequence identities between $LeuT_{Aa}$ and NNS proteins of about 30% in the TM regions were found by Yamashita et al.[12] The next computational challenge is to predict the orientation of the cognate substrate, 5-HT, in the binding cavity of the produced homology models of hSERT. Over the past decade, molecular docking has developed into a method of great use in medicinal chemistry,[32,33] and it works well in predicting the structure of the bound ligand in the protein, especially if a consensus docking approach is utilized.[34] However, so far molecular docking is not very good at predicting accurate binding affinities by use of the scoring functions, and more advanced methods must be applied.[35] Recently, it has been shown that molecular docking to homology models[36] of a protein is a good choice in virtual screening studies when no structure of the target is available. Some care must be taken, however, especially related to the orientation and flexibility of amino acid side chains lining the binding cavity. The binding cavity in the homology models of hSERT is expected to be rather tight for the larger substrate in hSERT compared to the leucine substrate in $LeuT_{Aa}$. This is partly overcome by the fact that some of the amino acids lining the binding cavity of hSERT are smaller than those in $LeuT_{Aa}$, thereby giving more space for 5-HT to fit. To further allow for a flexible binding cavity in order to accommodate 5-HT, we included protein flexibility by using the newly developed induced fit docking (IFD) methodology.[37] This protocol is among the first methods for including some degree of protein flexibility during a molecular docking simulation.

In this study we present a systematic exploration of the hSERT binding site and outline a preferred binding mode of 5-HT as obtained from IFD computations into carefully selected homology models of hSERT. The obtained models for ligand−protein interactions were challenged by the PaMLAC approach using 18 tryptamine analogues, Chart 1A, against wild type (wt) hSERT and 13 rationally chosen single point mutated transporters.

Chart 1. (A) 5-HT and 17 Analogues Used in the PaMLAC Studies. Numbering of Important Atoms in the Indole Ring Is Indicated on 5-HT. (B) Selected Drugs Targeting hSERT; β-CIT = 2β-2-carboxymethoxy-3-(4-[^{125}I]iodophenyl)tropane

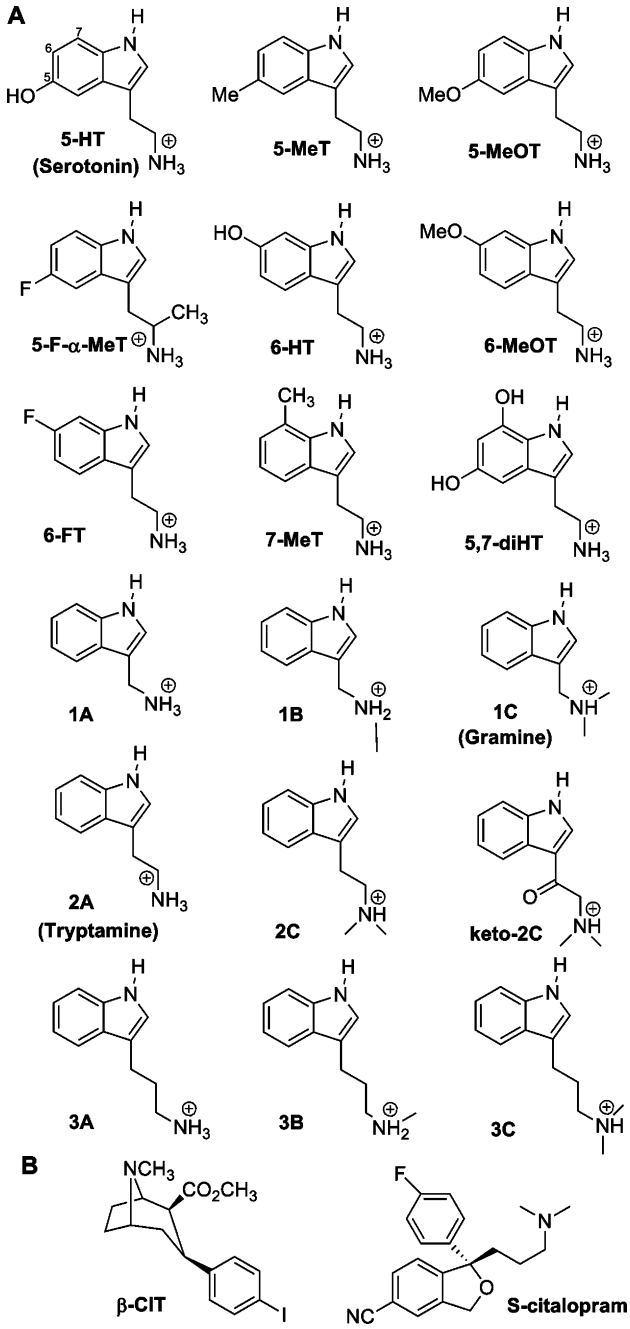

2. Computational Methods

2.1. Sequence Alignment. The amino acid sequence for hSERT was acquired from the UniProt Database,[38] accession number P31645. The sequence of $LeuT_{Aa}$ was extracted from pdb-entry code 2A65,[12] downloaded from the Protein Data Bank.[39] The long intracellular N-terminal of hSERT was not included in the homology modeling, only residues 79−630 covering the 12 α-helixes with intervening loops

(32) Chen, H.; Lyne, P. D.; Giordanetto, F.; Lovell, T.; Li, J. *J. Chem. Inf. Model.* **2006**, *46*, 401−415.
(33) Cummings, M. D.; DesJarlais, R. L.; Gibbs, A. C.; Mohan, V.; Jaeger, E. P. *J. Med. Chem.* **2005**, *48*, 962−976.
(34) Yang, J.-M.; Chen, Y.-F.; Shen, T.-W.; Kristal, B. S.; Hsu, D. F. *J. Chem. Inf. Model.* **2005**, *45*, 1134−1146.
(35) Warren, G. L.; Andrews, C. W.; Capelli, A.-M.; Clarke, B.; LaLonde, J.; Lambert, M. H.; Lindvall, M.; Nevins, N.; Semus, S. F.; Senger, S.; Tedesco, G.; Wall, I. D.; Woolven, J. M.; Peishoff, C. E.; Head, M. S. *J. Med. Chem.* **2006**, *49*, 5912−5931.
(36) Kairys, V.; Fernandes, M. X.; Gilson, M. K. *J. Chem. Inf. Model.* **2006**, *46*, 365−379.
(37) Sherman, W.; Day, T.; Jacobson, M. P.; Friesner, R. A.; Farid, R. *J. Med. Chem.* **2006**, *49*, 534−553.
(38) The UniProt Consortium. *Nucl. Acids Res.* **2007**, *35*, D193−D197.
(39) Berman, H. M.; Battistuz, T.; Bhat, T. N; Bluhm, W. F.; Bourne, P. E.; Burkhardt, K., Feng, Z.; Gilliland, G. L.; Iype, L.; Jain, S.; Fagan, P.; Marvin J.; Padilla, D.; Ravichandran, V.; Schneider, B.; Thanki, N.; Weissig, H.; Westbrook, J. D.; Zardecki, C. *Acta Crystallogr., Sect. D: Biol. Crystallogr.* **2002**, *58*, 899−907.

Table 1. hSERT Homology Models Built Using Alignments A, B, and C. Structural and Energetic Data for the 15 Models Are Listed

homology model	Ramachandran plot (%)[a]	DOPE (kJ/mol)	distance D98(Oδ)–Na1 (Å)[b]	GlideScore (kcal/mol)[c]	volume of binding site (Å^3)
A-1	94.9	−78607	4.1		90.1
A-2	94.6	−78374			101.9
A-3	94.7	−78040	3.3		84.0
A-4	95.7	−78360	3.5	−6.6	128.0
A-5	94.7	−78627	3.3		100.9
B-1	93.8	−77388	3.3		46.6
B-2	93.5	−76433			67.6
B-3	94.0	−78284	3.2		36.9
B-4	94.6	−77728			67.6
B-5	94.4	−77268			61.4
C-1	95.3	−79159	4.2		62.4
C-2	94.4	−78962			114.2
C-3	95.3	−79844	3.3		115.2
C-4	94.9	−79205	3.3		68.0
C-5	96.4	−79703	3.0	−6.7	143.9

[a] Percentage of residues with psi- and phi-values in the "favored" or "most favored regions" of the Ramachandran plot. [b] Only distances <5.0 Å are included. [c] GlideScore computed for docking of 5-HT in a rigid protein in Glide 4.0 using the SP scoring function.

and the short C-terminal were included. Three alignments of the target sequence of hSERT to the template, $LeuT_{Aa}$, are evaluated. The first alignment, A, is based on an automatic alignment created in MODELLER (version 8.1),[40] which uses the align2d methodology.[41] Additional manual adjustments were performed to eliminate unwanted gaps in the produced alignment for hSERT and to incorporate knowledge from available experimental data placing Asp98[19] and Ala169,[20] in the binding site by iteratively evaluating the DOPE (Discrete Optimized Protein Energy) scores[42] after model building. Ile172 has been shown to be important for binding of inhibitors to hSERT,[20,21] and its sequence proximity to Ala169 also places this residue in the binding cavity. Ile172 corresponds to Val104 in $LeuT_{Aa}$ which is indeed placed in the hydrophobic part of the binding cavity in $LeuT_{Aa}$.[12] No further attempts were done to refine the extra- and intracellular loops or the C-terminal, since they are distant from the transmembrane region and the putative ligand binding cavity (more than 20 Å), which is the focus of the present study, and thus are probably not affecting the binding of the substrate. The second alignment, B, was published with the $LeuT_{Aa}$ structure[12] and is used for generating the second set of homology models of hSERT. The third alignment, C, stems from a study by Beuming et al.[25] where experimental data was included for all known proteins in the NNS family to propose a detailed alignment.

2.2. Model Building. Five homology models, 1−5, were built for each of the three alignments, A-C, using MODELLER in stand-alone mode and default settings.[40] The produced 15 homology models, A1−5, B1−5, and C1−5, were evaluated by visual inspection (with respect to reproducing the protein backbone in the 12 TM helices, especially the kinks in TM1 and TM6) and by quantitative examinations through the Objective Function, DOPE scores, the volume of the binding site, and sterical features through Ramachandran plots (Table 1). The MODELLER Objective Function describes how well the model fits with all the input structural data,[43] and the DOPE-score[42] evaluates, per residue basis, the quality of the model against the template. The objective function and DOPE scores are energetic measurements and should thus both be as low as possible.[42,43] Stereochemical features of the obtained models were examined from Ramachandran plots generated in VMD 1.8.4 using the ramaplot plugin, version 1.0.[44] As the Ramachandran coordinates are optimized during the homology modeling procedure, it is obvious that the models with lowest DOPE score and objective function within one sequence alignment will have the best possible Ramachandran plots. In this way, the different alignments can be evaluated by comparing the computed Ramachandran scores; the better the alignment, the more favorable Ramachandran plots are expected. The volume of the binding cavity was measured by the Molegro Virtual Docker suite of programs, using the solvent accessible surface method with a maximum of 25 cavities per model.[45] Sodium ions were included by manual placement in the same relative place as they are located in the $LeuT_{Aa}$ structure. A chloride ion was manually inserted between residues Tyr121, Ser336, Asn368, and Ser372 in a few models (please see Supporting Information). The four residues and the Cl^- ion were minimized in MacroModel version 9.1[46] with the OPLS force field.

2.3. Ligand Modeling. 5-HT was drawn in Maestro[46] as charged on the primary amino group and minimized with the OPLS 2005 force field as implemented in MacroModel 9.1[46] for 10 000 steps of conjugate gradient iterations or until convergence, according to default settings.

2.4. Docking. Initial docking of 5-HT in the 15 homology models of hSERT was performed with Glide[47,48] version 4.0 using standard procedures.[46] This docking, with a rigid protein and a flexible ligand, was generally performed with the default standard precision (SP) scoring function in Glide;[47] however, the Glide extra precision (XP) scoring function[49] was tested for two models to evaluate if the special extra terms in this scoring function is of importance for this particular protein−ligand system. The binding site was defined from two residues (Asp98 and Ile172) which make up the two ends of the binding cavity parallel to the membrane plane.

2.5. Induced Fit Docking. To fully explore the concerns about flexible amino acid side chains when performing molecular docking simulations into homology models, we decided to include protein flexibility in the docking protocol using one homology model of hSERT from each alignment. Models of hSERT that allowed docking of 5-HT into a rigid protein were chosen for alignments A and C, whereas for B, where no poses were generated during normal docking, the homology model with the best energy scores and an interaction between Na1 and Asp98 was selected for further evaluation, resulting in selection of homology models A-4, B-3, and C-5 for further calculations. The IFD protocol[37,46] from Schrödinger Inc. that combines Glide 4.0[46] and Prime 1.5[46] was employed for docking of 5-HT into hSERT allowing for protein flexibility.[37,50] The IFD workflow consists of three steps. First, the ligand is docked flexibly into a rigid protein with a soft Van der Waals potential, thereby allowing for some steric clash. During this step it is possible to make point mutations of highly flexible residues to alanine, to artificially create more room and secure that at least a few poses of the protein−ligand complex are generated; this was not necessary for introducing 5-HT into the hSERT binding site. In the second step during an IFD workflow the protein is optimized, using Prime, within 5.0 Å of the ligand poses from the first step, and if any residues were mutated in the first step, they are reintroduced. The final step is a redocking of the ligand into the relaxed protein binding cavity, where normal Van der Waals terms are used. Either the SP or XP scoring function can be applied in the last step. The final scoring from an IFD calculation is the computed GlideScore (SP or XP) reflecting the interaction between the protein and the ligand. Another reported

(40) Sali, A.; Blundell, T. L. *J. Mol. Biol.* **1993**, *234*, 779−815.
(41) Sanchez, R.; Sali, A. *Proc. Natl. Acad. Sci. U.S.A.* **1998**, *95*, 13597−13602.
(42) Eramian, D.; Shen, M.; Devos, D.; Melo, F.; Sali, A.; Marti-Renom, M. A. *Protein Sci.* **2006**, *15*, 1653−1666.
(43) Eswar, N.; John, B.; Mirkovic, N.; Fiser, A.; Ilyin, V. A.; Pieper, U.; Stuart, A. C.; Marti-Renom, M. A.; Madhusudhan, M. S.; Yerkovich, B.; Sali, A. *Nucl. Acids Res.* **2003**, *31*, 3375−3380.
(44) Humphrey, W.; Dalke, A.; Schulten, K. *J. Mol. Graph.* **1996**, *14*, 33−38.
(45) Thomsen, R.; Christensen, M. H. *J. Med. Chem.* **2006**, *49*, 3315−3321.
(46) Schrödinger, LLC, 2006.
(47) Friesner, R. A.; Banks, J. L.; Murphy, R. B.; Halgren, T. A.; Klicic, J. J.; Mainz, D. T.; Repasky, M. P.; Knoll, E. H.; Shelley, M.; Perry, J. K.; Shaw, D. E.; Francis, P.; Shenkin, P. S. *J. Med. Chem.* **2004**, *47*, 1739−1749.
(48) Halgren, T. A.; Murphy, R. B.; Friesner, R. A.; Beard, H. S.; Frye, L. L.; Pollard, W. T.; Banks, J. L. *J. Med. Chem.* **2004**, *47*, 1750−1759.
(49) Friesner, R. A.; Murphy, R. B.; Repasky, M. P.; Frye, L. L.; Greenwood, J. R.; Halgren, T. A.; Sanschagrin, P. C.; Mainz, D. T. *J. Med. Chem.* **2006**, *49*, 6177−6196.
(50) Teague, S. J. *Nat. Rev. Drug Discovery* **2003**, *2*, 527−541.

Table 2. IFD Simulations of 5-HT in the Three Homology Models of hSERT

setup	homology model	sodium	binding site	scoring function	poses	cluster1	cluster2	cluster3	outlier
1	A-4	none	D98, I172	SP	7	2	2	2	1
2	A-4	Na1	D98, I172	SP	10	5	4	1	
3	A-4	Na2	D98, I172	SP	9	4	1	3	1
4	A-4	Na1, Na2	D98, I172	SP	9	6	3		
5	A-4	Na1	5-HT[a]	SP	9	7	2		
6	A-4	Na1, Na2	D98, I172	SP/XP[b]	7	4	2		1
7	B-3	none	D98, I172	SP	3[c]				1
8	B-3	Na1	D98, I172	SP	3[c]				
9	B-3	Na2	D98, I172	SP	6[c]				
10	B-3	Na1, Na2	D98, I172	SP	1[c]				
11	B-3	Na1, Na2	D98, I172	SP/XP[b]	1[c]				
12	C-5	none	D98, I172	SP	9	7		2	
13	C-5	Na1	D98, I172	SP	10	7		2	1
14	C-5	Na2	D98, I172	SP	10	7		3	
15	C-5	Na1, Na2	D98, I172	SP	8	6	1	1	
16	C-5	Na1	5-HT[a]	SP	7	6		1	
17	C-5	Na1	5-HT[d]	SP	10	10			
18	C-5	Na1, Na2	D98, I172	SP/XP[b]	6	5		1	
				total	125	76	15	16	5

[a] 5-HT as docked in the rigid homology model with the SP scoring function was used for definition of the binding site in IFD. [b] The XP-scoring function is used in the redocking step of the IFD simulation. [c] All but one pose in model B-3 are placed outside the binding cavity. [d] 5-HT as docked in the rigid homology model with the XP scoring function was used for definition of the binding site in IFD.

score is the IFDScore, which is an empirical measure of the energetics of the total protein−ligand complex. It is a sum of the reported G-score and 5% of the Prime energy, which is a force field-calculated energy of the protein after the refinement in step two of the IFD workflow.[37] Different setups were created examining the effect of the three homology models, the presence of the two sodium ions, the definition of the binding site, and the scoring function utilized in step three of IFD. In total, 18 different IFD calculations were carried out as listed in Table 2.

3. Experimental Methods

3.1. Ligand Synthesis. Compounds 1C (Gramine), 2A (Tryptamine), keto-2C, 5-F-α-MeT, 5-HT, 5-MeT, 5-MeOT, 5,7-diHT, 6-FT, 6-MeOT, and 7-MeT were purchased from Sigma-Aldrich, 1A from Maybridge, and 6-HT from National Institute of Mental Health's Chemical Synthesis and Drug Supply Program; all were used as received. Compounds 1B, 2C, 3A, 3B, and 3C were synthesized by us (see the Supporting Information).

3.2. Site-Directed Mutagenesis. Site-directed mutagenesis was performed using the method of mismatched complimentary primer pairs in a polymerase reaction with Phusion (Finnzyme) using hSERT in the pCDNA3 (Invitrogen) vector as template. Mutants were verified and checked for unwanted secondary mutations by automated DNA sequencing using Big Dye 3.1 (Applied Biosystems) chemistry. For further details see the Supporting Information.

3.3. Cell Culture. HEK-293 MSR cells (Invitrogen) were cultured as monolayer cultures in DMEM (BioWhitaker) supplemented with 10% FCS (Gibco Life Technologies), 100 U/mL penicillin, 100 μg/mL streptomycin (BioWhitaker), and 6 μg/mL of Geneticin (Invitrogen) at 95% humidity and 5% p(CO_2) at 37 °C. Cells were detached from the culture flasks by Versene (Invitrogen) and trypsin/EDTA (BioWhitaker) treatment for subculturing or seeding into microtiter plates.

3.4. Uptake Assay. Measurement of 5-HT uptake was performed as described by Larsen et al.[20] HEK-293 MSR cells (Invitrogen) were used instead of COS-1 cells. For further details see the Supporting Information.

4. Results

4.1. Modeling. 4.1.2. Sequence Alignment and Model Building. A total of 15 homology models (Table 1) were built in MODELLER[40] from three different alignments: one developed by us (A) and two that have previously been published, B[12] and C.[25] A figure of the three alignments against each other and the $LeuT_{Aa}$ template is included in the Supporting Information. Our alignment was manually refined to remove gaps from within the transmembrane segments and to place Asp98,[19] Ala169,[20] and Ile172[20,21] in the putative binding site. This was a procedure including several iterations of (i) refining the alignment, (ii) building models, (iii) comparing DOPE scores[42] between template and target for individual residues, and (iv) visually inspecting the binding cavity. When comparing the DOPE score for individual residues between the template and the model, a high similarity generally implies a good model, allowing us to further refine the alignment. In the final alignment, A, the highest differences in DOPE scores were located in loops outside the membrane layer. These have not been further refined at this point since they are located more than 20 Å from the binding pocket; therefore, their detailed structure is not expected to influence ligand binding. Figures of DOPE scores for the three alignments are included in the Supporting Information. The three alignments show sequence identities for hSERT against $LeuT_{Aa}$ of 23%, 20%, and 19%, respectively, for the full protein and about 28% sequence identity in the TM regions. The differences between the three alignments are located in α-helices TM4, TM5, TM9, and TM12 all of which are located distant from the binding cavity. If conservative mutations of amino acids are considered, sequence similarities of 55−56% are observed between $LeuT_{Aa}$ and hSERT. Within 5 Å of the binding site the identity is even higher (19 out of 25 residues = 76%), while more differences are found in the non-membrane embedded loop regions. Since the $LeuT_{Aa}$ structure was solved to 1.65 Å[12] and computed sequence identity numbers between template and target are around 30%, one can expect the resulting homology models to be of a good quality with around 2 Å deviations between Cα-atoms of the models and the true native structure of hSERT.[31]

The structures of the 15 homology models are highly similar and all include the important feature found in the $LeuT_{Aa}$ structure;[12] helices TM1 and TM6 are unwound in the middle to allow for substrate binding in an occluded binding site between helices TM1, TM3, TM6, and TM8 (Figure 1). Because

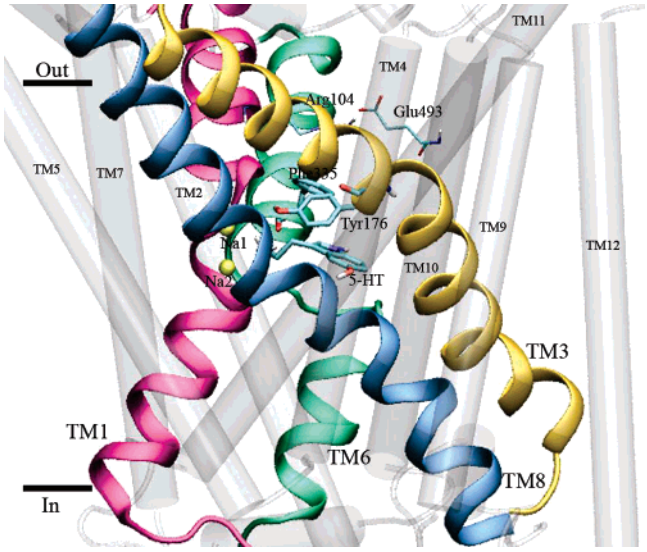

Figure 1. Structure of the hSERT homology model showing helices TM1, TM3, TM6, and TM8 around the binding site together with the two sodium ions from the $LeuT_{Aa}$ structure and 5-HT. The binding site is closed toward the extracellular lumen by an aromatic lid (residues Tyr176 and Phe335) and a salt bridge (Arg104 and Glu493). Helices farther away from the binding site are shaded.

of the very high similarity between the models neither the MODELLER Objective Function[40] (not shown) nor the DOPE scores[42] can be employed to directly distinguish their accuracy. However, it is interesting to note that the five homology models generated from alignment B generally exhibit the smallest binding cavities, the poorest DOPE scores, and the lowest number of residues in the allowed parts of the Ramachandran plots. Furthermore, only two of the five homology models from alignment B show the expected coordination of Asp98 to Na1, compared to four out of five models from alignment A and C.

Ramachandran plots (data in Table 1) reveal that an overall favorable stereochemistry is found in all models implying that the alignments are in accordance with the secondary structure elements. The residues occupying disallowed areas of the conformational space are either glycine residues or they are located in the extra- and intracellular loops, consistent with their observed flexible nature. One residue does stand out here, namely Asp98 with (φ,ψ) around ($-150°$, $-150°$) in all models. However, Asp98 is located in the unwound part of TM1 in the binding site and is thus not obliged to a particular conformation to maintain any secondary structure.

4.1.2. Initial Docking and Selection of Homology Models for IFD. The ligand binding site in the hSERT models is generally too small for direct docking of 5-HT in the 15 homology models using Glide.[46] This was also observed by others[25,26] who had to manually place the ligand in the binding cavity by superimposition and subsequent minimization, sometimes imposing rather severe constraints. In contrast, we succeeded in using molecular docking for placing 5-HT in the binding cavity in two of the 15 homology models of hSERT, A-4 and C-5, by using Glide 4.0[46] with default settings. These are the two models with the largest cavities. However, rather poor GlideScores were computed. Because of the possibility of directly docking 5-HT into models A-4 and C-5, these two models were selected for further IFD studies. Of the five homology models from alignment B only two (B-1 and B-3) allow Asp98 to interact with Na1 as suggested by Yamashita et al.[12] Since B-3 has a lower DOPE score than B-1 and no significant differences could be detected around the binding cavities of the two models, B-3 was chosen for the IFD studies, resulting in one model per alignment. The three alignments were identical around the binding cavity, which indicates that the differences in the measured volumes must originate from differences in the side chain positioning, as during the building of the homology models in MODELLER, no major backbone manipulations away from the template structure is possible. Since IFD is employed in the next stage of our theoretical prediction of a binding geometry of 5-HT in hSERT, the exact rotamer state of the side chain is not maintained during the docking simulation, and it may thus be less important which homology model was initially chosen for each of the three alignments, the important feature being that the ligand can be docked in the first step of the IFD workflow.

4.1.3. Induced Fit Docking. IFD[37,46] of 5-HT into hSERT was performed to compensate for the rather small binding site in the homology models in an unbiased fashion that is likely to be consistent with natural protein dynamics upon ligand binding. To examine the favored binding mode of 5-HT, several aspects were examined through 18 different setups as listed in Table 2, thereby introducing a kind of consensus scoring scheme for the study. The preference of the two sodium ions from the $LeuT_{Aa}$ structure[12] was examined in four setups for each homology model, setups 1−4, 7−10, and 12−16, respectively. The influence of a predocked 5-HT was tested in setups 5, 16, and 17, and the effect of the Glide XP scoring function[49] in the redocking of ligands was explored in one setup for each homology model (6, 11, and 18). Since protein flexibility is included in IFD, up to 10 poses were written from each setup, entailing a total of 125 poses of 5-HT binding in hSERT out the theoretical maximum of 180 poses. Computed docking scores (IFDScore and GlideScore) for all poses are tabulated in the Supporting Information.

The results reveal that the presence of none, one, or two sodium ions did neither significantly influence the statistics of the docking nor the structural features of the generated poses; by comparison of the statistics from setup 1−4, 7−10, and 12−15, respectively, for alignments A, B, and C, Table 2, it is clear that the major differences in results from the setups with varied sodium ion inclusion are found in the computed Prime energies, which reveal the energy of the protein. The results (see Supporting Information) indicate that the Na2 seems to be more important than Na1 in stabilizing the protein and supports the suggestion from Yamashita et al. that one of the sodium ions may be structural, while the other is transported.[12]

It was possible to group 107 of the poses into three binding clusters, each defined by the position and orientation of the 5-HT indole ring (Figure 2). The statistics of the division of poses into clusters as well as the total number of poses from each setup are included in Table 2. Only one of the poses from model B-3 has 5-HT located in the binding site; the other 13 poses all have 5-HT positioned in the extracellular vestibule of the transporter. They lie outside the aromatic lid, consisting of Tyr176 and Phe335, in the space normally occupied by a salt bridge, Arg104···Glu493 (corresponding to Arg30···Asp404 in $LeuT_{Aa}$), which is therefore not present in these poses. The poses with 5-HT located in the extracellular vestibule have the ligand in random orientations, and at a first glance they do not seem

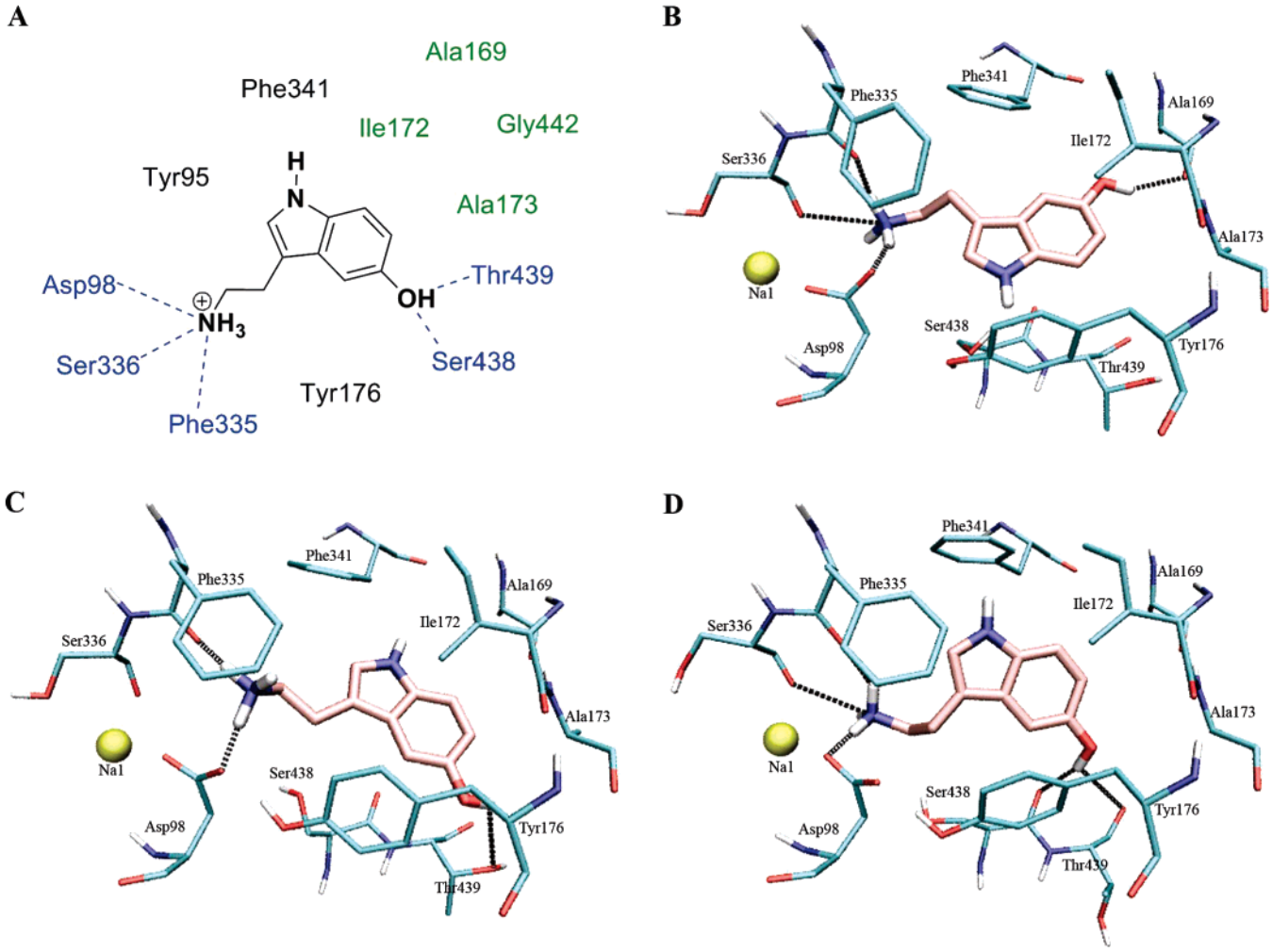

Figure 2. Orientation of 5-HT in the hSERT binding site. (A) Schematic representation of the binding site with possible hydrogen bonds shown in blue and the aliphatic "bottom" of the binding site in green. Coordination of 5-HT in the three clusters identified from IFD are shown (B) cluster 1, setup 5, (C) cluster 2, setup 5, and (D) cluster 3, setup 18. Carbon atoms of 5-HT are shown in pink while those in the protein are colored cyan. Putative hydrogen bonds to 5-HT are included in the three IFD clusters.

to be relevant compared to the recently published structures of $LeuT_{Aa}$ with TCAs bound in the extracellular vestibule.[13,14] It should be noted here that the identified imipramine binding site in $LeuT_{Aa}$ has been suggested to be a secondary site, of no or little importance related to the functioning of the NSSs.[51] Imipramine has been shown to be a competitive inhibitor of transport of 5-HT in hSERT, and it seems unlikely that the primary binding site of the tricyclic amines should be so distant from Ile172, which has been shown to be important in inhibitor binding.[20,21] Also, kinetic evidence for hSERT has suggested that a secondary low-affinity binding site for imipramine exists that is different from the inhibitory site.[52,53] In line with these arguments from the literature it is interesting to observe that the computed docking scores of poses in the extracellular vestibule after IFD were much less favorable than those placing 5-HT in the putative central binding pocket (see numbers in the Supporting Information). In this study we focus on the primary binding site; thus, the poses with 5-HT in the vestibule were excluded from further analysis. All 14 poses from model B-3 were consequently excluded, since the single pose in the binding site has very poor docking scores and represents a structural outlier compared to the three identified clusters. An additional four poses from models A-4 and C-5 were similarly found to represent structural outliers and were not included in the analysis. All poses from 5-HT docking in A-4 and C-5 with IFD were placed in the putative biding site and none in the vestibule. Furthermore, it should be noted that the two poses generated in the initial rigid protein docking belongs to the clusters identified in IFD. IFD studies with setup 4, 6, 15, and 18 were subsequently repeated with inclusion of a chloride ion in the recently proposed anion binding site.[24,30] Results from these simulations are equivalent to those described in Table 2, and the chloride ion, thus, does not seem to be affecting the binding of 5-HT. This is probably due to the distance (around 9 Å) between the 5-HT amino group and the chloride ion and the presence of Na1 between the two groups. Results for these simulations are tabulated in the Supporting Information.

4.1.4. Analysis of 5-HT Binding Clusters. Figure 2A shows a schematic representation of the hSERT binding site. Parallel to the membrane plane, Asp98 anchors all 5-HT poses in one end while the other end (the 5-HT C6-position) is located near Ala173 in a pocket that is generally hydrophobic, but includes

(51) Rudnick, G. *ACS Chem. Biol.* **2007**, *2*, 606−609.
(52) Wennogle, L. P.; Meyerson, L. R. *Eur. J. Pharmacol.* **1982**, *86*, 303−307.
(53) Plenge, P.; Mellerup, E. T. *Eur. J. Pharmacol.* **1985**, *119*, 1−8.

Table 3. Mean K_i (μM) and 95% Confidence Intervals (in brackets) for Inhibition of [^{3}H]-5-HT Uptake from at Least Three Independent Experiments for 18 Tryptamine Analogues against wt hSERT and 13 Single Point Mutants

substrate analogue	wt hSERT	Ala173Cys	Ala173Ser	Ala173Thr	Ala173Asp	Ala173Met	Ala173Leu
1A	123 [59−250]	112 [14.5−870]	137 [12.3−1500]	147 [5.6−3800]	60 [4.8−740]	43 [3.3−570]	18.1 [9.6−34]
1B	22 [13.7−37]	13.2 [7.2−24]	9.8 [1.28−75]	15.7 [4.7−52]	7.5 [2.8−20]	7.1 [2.5−20]	3.6 [1.52−8.3]
1C	15.7 [10.0−25]	9.0 [3.5−23]	7.5 [2.1−27]	9.0 [2.6−31]	4.7 [3.3−6.7]	3.2 [1.92−5.2]	2.1 [1.02−4.4]
2A	2.4 [1.05−5.3]	1.05 [0.55−1.98]	1.26 [0.40−4.0]	2.0 [1.51−2.8]	0.95 [0.46−1.95]	1.94 [0.95−3.9]	4.6 [0.32−67]
2C	2.8 [1.19−6.5]	1.13 [0.05−24]	0.95 [0.031−29]	1.25 [0.028−56]	0.43 [0.035−5.3]	0.63 [0.025−15.7]	0.82 [0.33−2.0]
keto-2C	11.5 [7.0−18.6]	5.5 [0.82−37]	4.9 [0.168−140]	9.9 [3.4−29]	3.2 [0.31−33]	9.3 [3.02−28.4]	2.7 [1.93−3.7]
3A	0.95 [0.5−1.81]	0.81 [0.37−1.76]	1.10 [0.166−7.4]	4.2 [1.95−9.2]	0.66 [0.049−8.8]	1.74 [1.11−2.7]	0.91 [0.74−1.11]
3B	0.36 [0.07−2.0]	0.26 [0.0185−3.6]	0.27 [0.024−3.0]	0.74 [0.0182−30]	0.101 [0.0134−0.7 6]	0.31 [0.032−3.0]	ND[a]
3C	0.74 [0.54−1.02]	0.66 [0.35−1.25]	0.75 [0.21−2.7]	1.94 [0.136−28]	0.31 [0.135−0.72]	0.84 [0.31−2.3]	1.87 [1.28−2.8]
5-F-α-MeT	0.42 [0.23−0.77]	0.69 [0.46−1.03]	0.47 [0.22−1.03]	0.55 [0.25−1.23]	0.56 [0.40−0.80]	0.86 [0.61−1.22]	0.7 [0.35−1.4]
5-HT	0.92 [0.51−1.65]	1.54 [0.65−3.6]	1.30 [0.38−4.5]	5.2 [3.2−8.3]	2.5 [2.2−2.9]	7.5 [3.8−14.6]	16.5 [6.6−41]
5,7-diHT	42 [18.3−96]	46 [16.0−133]	26 [16.0−42.5]	18.9 [10.4−34]	81 [27−240]	185 [99−350]	280 [86−890]
5-MeT	18.4 [10.7−31]	10.5 [4.7−24]	11.3 [2.6−50]	12.9 [8.1−21]	11.2 [4.8−26]	4.3 [4.0−4.7]	2.6 [2.3−3.0]
5-MeOT	56 [37−83]	22 [9.4−52]	21 [7.7−57]	21 [18.2−24]	13.1 [4.8−36]	4.5 [3.5−5.7]	4.6 [2.3−9.2]
6-HT	42 [27−64]	17.0 [9.1−32]	2.1 [1.78−2.4]	2.2 [0.82−5.7]	16.3 [9.2−29]	9.1 [4.8−17.3]	9.8 [3.3−29]
6-MeOT	2.6 [2.1−3.3]	4.4 [3.9−5.0]	2.8 [1.75−4.4]	9.8 [5.4−16.1]	7.9 [5.3−11.8]	1.87 [1.30−2.7]	1.86 [0.8−4.4]
6-FT	0.21 [0.11−0.4]	0.42 [0.32−0.55]	0.40 [0.163−0.96]	0.78 [0.60−1.02]	1.08 [0.57−2.0]	0.67 [0.33−1.36]	0.43 [0.26−0.71]
7-MeT	0.37 [0.26−0.55]	0.40 [0.169−0.94]	0.38 [0.25−0.57]	0.37 [0.091−1.47]	0.30 [0.21−0.44]	0.34 [0.093−1.28]	0.32 [0.07−1.37]

substrate analogue	Asp98Glu	Tyr175Phe	Tyr176Phe	Thr439Ala	Thr439Ser	Thr439Val	Ala169Ile
1A	105 [35−320]	146 [16.7−1270]	74 [3.7−1500]	17.7 [13.9−22]	51 [15.4−167]	55 [7.2−430]	105 [30−370]
1B	13.3 [2.9−61]	13.4 [6.9−26]	22 [11.7−40]	5.4 [2.1−13.8]	9.4 [5.0−17.8]	8.7 [2.8−27]	26 [6.9−94]
1C	1.19 [0.63−2.3]	5.6 [1.03−31]	32 [8.2−127]	5.3 [4.1−6.9]	3.2 [1.87−5.4]	6.2 [2.4−16.3]	9.1 [7.0−11.8]
2A	0.37 [0.14−0.98]	0.84 [0.138−5.1]	4.8 [2.5−8.9]	1.41 [0.182−10.9]	0.83 [0.60−1.13]	2.0 [0.31−13.1]	7.6 [1.41−41]
2C	1.42 [0.60−3.4]	1.47 [0.153−14.1]	3.7 [0.38−36]	2.2 [0.80−5.9]	1.81 [0.61−5.4]	1.74 [0.40−7.5]	2.1 [1.27−3.5]
keto-2C	2.8 [1.25−6.1]	7.1 [1.81−28]	22 [13.3−37]	4.2 [2.2−8.0]	5.6 [5.0−6.2]	3.4 [0.88−12.9]	28 [14.1−44]
3A	0.65 [0.22−1.92]	0.53 [0.118−2.4]	4.1 [1.18−14.3]	0.68 [0.32−1.46]	1.84 [1.00−3.4]	0.39 [0.075−2.04]	2.6 [1.41−4.9]
3B	0.31 [0.068−1.43]	0.37 [0.038−3.5]	0.30 [0.026−3.4]	ND	ND	ND	ND
3C	0.44 [0.128−1.51]	0.98 [0.38−2.6]	0.80 [0.153−4.2]	0.078 [0.0130−0.4 6]	0.40 [0.042−3.9]	0.26 [0.0181−3.8]	4.8 [1.22−18.5]
5-F-α-MeT	0.107 [0.025−0.46]	0.21 [0.10−0.44]	0.79 [0.48−1.3]	0.088 [0.051−0.15 1]	0.10 [0.0081−1.1 3]	0.183 [0.035−0.97]	0.92 [0.69−1.22]
5-HT	0.64 [0.25−1.65]	0.43 [0.10−1.93]	1.35 [0.78−2.3]	3.7 [1.08−12.6]	0.62 [0.3−1.28]	1.15 [0.24−5.5]	3.8 [1.98−7.2]
5,7-diHT	4.0 [0.119−133]	9.7 [4.6−20]	37 [15.9−88]	179 [65−500]	22 [1.12−420]	68 [8.3−560]	520 [120−2300]
5-MeT	3.3 [2.5−4.4]	10.1 [1.40−73]	40 [25−64]	1.36 [0.191−9.7]	21 [4.2−97]	6.9 [1.79−27]	6.4 [2.9−14.5]
5-MeOT	ND	26 [6.4−103]	47 [35−62]	2.55 [0.57−11.5]	25 [12.4−49]	28 [7.0−111]	6.6 [2.2−19.7]
6-HT	ND	17.8 [8.3−38]	52 [22−124]	12.0 [7.1−20]	12.3 [0.93−162]	24 [6.0−98]	57 [31−105]
6-MeOT	1.36 [1.18−1.58]	0.76 [0.50−1.17]	3.9 [1.80−8.6]	0.40 [0.029−57]	1.23 [0.21−7.3]	1.63 [0.88−3.0]	1.82 [1.2−2.8]
6-FT	0.126 [0.022−0.73]	0.141 [0.043−0.47]	0.28 [0.173−0.46]	0.099 [0.028−0.35]	0.079 [0.022−0.29]	0.158 [0.036−0.71]	0.30 [0.17−0.53]
7-MeT	ND	0.122 [0.048−0.31]	0.34 [0.161−0.71]	0.152 [0.058−0.40]	0.077 [0.0085−0.7 0]	0.175 [0.021−1.47]	1.80 [0.79−4.1]

[a] ND: Not determined.

some hydrophilic character. Residues Tyr176 and Phe335, constituting the aromatic lid, are located on the extracellular side of the bound ligand. The 5-HT···Asp98 interaction is either purely ionic or has an additional hydrogen bond character, depending on the distances (tabulated in the Supporting Information). The difference between the clusters is an approximately 180° rotation of the indole ring in the binding site (Figure 2B−D). In cluster 1 the indole N−H points toward Tyr176, while it faces Phe341 in clusters 2 and 3; in cluster 2 it points toward the edge of the Phe341 aromatic ring while it is orthogonal to and points directly toward the center of the aromatic ring in cluster 3. The only difference between clusters 2 and 3 is, thus, a parallel displacement of the indole ring positioning it approximately 2−3 Å deeper into the binding pocket in cluster 2. The retained interaction with Asp98 can be rationalized by different conformations of the 5-HT ethylamine side chain; in cluster 2 it is elongated while it is less extended in cluster 3 (Figure 2C and 2D). Because of the high structural similarity between the binding of 5-HT in clusters 2 and 3, they are referred to as one single binding mode versus another binding mode represented by cluster 1, leading to two possible orientations of 5-HT in the hSERT binding site differing in the indole ring orientation. Additional interactions to 5-HT in the binding site includes a large number of hydrophobic interactions as well as possible hydrogen bonds to the 5-hydroxyl group: In cluster 1 a hydrogen bond to the Ala169 carbonyl oxygen can be found while there is a possible hydrogen bond to Thr439 in clusters 2 (hydroxyl group) and 3 (carbonyl) and another possible interaction to Ser438 (carbonyl) in cluster 3, as indicated in Figure 2.

4.2. Biochemistry. 4.2.1. PaMLAC Study of 5-HT in hSERT. In order to be able to confirm the predicted binding of 5-HT in hSERT and to discriminate between the two orientations found with IFD (cluster 1 and clusters 2/3, respectively), we undertook a SAR study measuring the binding affinities of a battery of substituted tryptamines, Chart 1A, toward wt hSERT and 13 single point mutants of the protein. The location and nature of the mutations were selected in a way that would allow us to achieve experimental data that would either challenge or support the two orientations of 5-HT as predicted from the IFD simulations. All data are listed in Table 3. Below we present the studied protein−ligand interactions one by one and analyze the effects on binding affinities of essential single point mutations according to the PaMLAC paradigm, starting with Asp98 and Ala173 to examine the identical features of the two orientations, establishing the position of the ligand axis in the binding site. The rotation around the axis, as revealed in the three clusters, is then evaluated by mutations of Ala169 and Thr439.

4.2.2. Interpretation of Experimental Data. Assumptions. Conclusions about 5-HT binding in hSERT by the use of tryptamine analogues and transporter mutants in biochemical assays rest upon the assumptions that (a) tryptamines bind to the same site as 5-HT, (b) the mutations do not alter the overall binding orientation but solely affect the binding affinity, (c) mutant hSERTs are not subject to changes in the conformational equilibrium of the transporter that affects binding of 5-HT and tryptamine analogues differently, and (d) observed K_i values primarily reflect initial binding affinity and not K_M.

The assumption that the tryptamine analogues bind to the same site as 5-HT appears reasonable since they are competitive inhibitors of 5-HT transport.[54] Additionally, the observation that our models are able to predict an interaction between both ends of the ligand with both ends of the putative binding site, which can be supported experimentally (*vide infra*) under the PaMLAC paradigm, justifies that the tryptamines bind to hSERT in a very similar fashion.

If mutations in hSERT or substitutions on the ligand were severe it is possible that the ligand might assume another orientation in the binding site. Such a situation could occur if, e.g., an acidic residue (apart from Asp98) is mutated into the binding cavity introducing a competition for interaction with the positively charged nitrogen atom of the tryptamines. Results from IFD suggest that changes in the ligand orientation would initially manifest itself as a rotation of the indole ring, as these are the only poses observed. However, if an aspartate or glutamate residue is introduced in the hydrophobic bottom of the cavity by mutation of either Ala169, Ile172, Ala173, or Gly442, one can speculate that such a dramatic mutation could cause a longitudinal swap of the ligand. We do not detect any signs of such changes of ligand orientation in our experimental data and therefore believe that variations in the substitution pattern are neither sufficient to flip the indole ring nor to revert the ligand axis.

4.2.3. Experimental Test of Salt Bridge between Asp98 and 5-HT. The acidic side chain of Asp98 is predicted to form a salt bridge with the positively charged amine of 5-HT.[12] Asp98 is indeed very sensitive to mutagenesis, underscoring the importance of this residue for transporter function. Asp98Gly, Asp98Ala, and Asp98Asn mutants were all found to be inactive with regards to uptake of 5-HT and binding of β-CIT and [^{3}H]-S-citalopram (data not shown; for structures see Chart 1B). Only the Asp98Glu mutant was active and is included in this study to elaborate on the elegant experiments with N-methylated tryptamines by Barker et al.,[19] addressing the existence of this putative salt bridge. We have extended their study by including tryptamine analogues that are not N-methylated and thus mimic the cognate substrate, 5-HT, more closely. Shortening the alkylamine chain, analogues 1A (123 μM) and 1C (15.7 μM) relative to 2A (2.4 μM) and 2C (2.8 μM), substantially reduces affinity for the wt transporter (Table 3). As stated in the PaMLAC approach, a measured loss of affinity when perturbing the substrate analogue must be followed by regaining some of the affinity by a single point mutant compensating for the chemical changes in the ligand. Indeed, the loss of affinity for the short tryptamines can be partially or fully rescued by simultaneously extending the side chain of Asp98 by mutating it to a glutamate, as is expected if the Asp98···ligand salt bridge is present. Furthermore, all tryptamines show improved binding affinities toward the Asp98Glu mutant, but 1A and 1C gain most. This can be interpreted as the alkylamine group in 1A and 1C that assumes an extended conformation to gain an interaction with Glu98, whereas the longer alkylamine chains most likely are found in a more folded conformation for the other analogues.

4.2.4. Exploration of Environment around the C6-Position of 5-HT. From the IFD simulations it was predicted that the 5-HT C6-position may provide a basis for an interaction with Ala173. We set up a series of PaMLAC experiments to test this hypothesis, and if true, to characterize the electronic nature of the protein near C6. Wild type hSERT allows some diversity in substitutions on C6 of the tryptamines; 6-MeOT (2.6 μM) and 6-FT (0.21 μM) are both well tolerated and have binding properties similar to 5-HT (0.92 μM) and tryptamine (2.4 μM), whereas 6-HT (42.0 μM) shows a drastically decreased affinity. A small hydrophobic pocket in the protein near C6 of the ligand thus seems likely. In accordance with the PaMLAC paradigm, we want to test this hypothesis by reverting the nature of the apparent hydrophobic interaction between C6 of the tryptamine analogues and the Ala173 side chain to create a novel interaction, thereby firmly establishing the existence of a direct ligand−protein contact point. The fact that a methoxy substituent at C6 can be accommodated without loss of affinity toward wt hSERT compared to tryptamine indicates that sufficient space exists around the C6 position of the ligands to allow for a mutation of the hydrophobic side chain of Ala173 to serine or threonine, both hydrophilic. This is expected to be harmful for the affinity of 6-MeOT. This pattern can be observed for Ala173Thr (9.8 μM) but (surprisingly) not for Ala173Ser (2.8 μM), see Table 3. This observation is difficult to directly explain; however, it may be related to the observation that in the IFD models the Ala173 side chain in wt hSERT is not pointing directly into the binding cavity (Figure 2). It rather occupies a more tangential orientation at the protein−ligand interface, and maybe the effect of the methyl group in Ala173Thr becomes important for orienting the hydroxyl group properly for interaction with the ligand. It can further be predicted that Ala173Ser and Ala173Thr may present a novel hydrogen-bonding partner to appropriate substituents of the C6-atom of tryptamine, if the hydroxyl group can indeed reach into the binding cavity. Hence, the poor affinity of 6-HT for wt hSERT is expected to improve for Ala173Ser and Ala173Thr if the orientation predicted from the IFD simulations is correct. This pattern is, indeed, observed with a 20-fold increase in affinity of 6-HT for Ala173Ser (2.1 μM) and Ala173Thr (2.2 μM) relative to wt hSERT (42 μM). This complementing mutation effectively restores the affinity of 6-HT to the same level as that of tryptamine for wt hSERT (2.4 μM), demonstrating a full reversal from the native hydrophobic interaction of the C6 hydrogen in tryptamine with Ala173 to a hydrophilic interaction of 6-HT with single point mutated proteins Ala173Ser or Ala173Thr. Having now established the two longitudinal anchor points of the ligand, we moved to experiments designed to probe the rotation of the ligand around this axis. This can be accomplished by identification of interaction partners with either the N−H bond of the indole ring or with substituents at the C5- or C7-positions of the tryptamine analogues.

(54) Adkins, E. M.; Barker, E. L.; Blakely, R. D. *Mol. Pharmacol.* **2001**, *59*, 514−523.

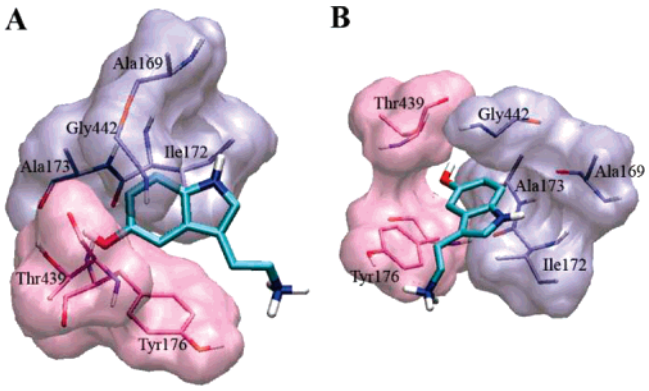

Figure 3. Two views, rotated by approximately 90°, of the two binding pockets around C5 (mauve) and C7 (ice-blue) of 5-HT displayed in cluster 2 (model A-4). Van der Waals surfaces of residues around the indole ring are shown.

4.2.5. Environment around the C5- and C7-Positions of 5-HT. The SAR data listed in Table 3 reveals some flexibility with respect to substituents at C5 of the tryptamine analogues toward wt hSERT; hydrogen, fluoro, or hydroxyl groups in this position result in very similar binding affinities with mean K_i values between 0.42 μM and 2.4 μM. On the other hand, hydrophobic substituents, such as methyl and methoxy groups, result in poor binding and elevated mean K_i values of 18.4−56 μM. This indicates that a small group is important, and some hydrophilic character is preferred (OH and F), however, not strictly required (H). For the C7-position of the tryptamine skeleton, a methyl substituent is favorable; 7-MeT binds equally well as 5-HT toward wt hSERT and 6-fold better than tryptamine (Table 3). The additional observation that placing a hydroxyl group at C5 and another at C7 at the same time, 5,7-diHT (42 μM), results in a poor binding compared to 5-HT (0.92 μM) strongly indicates that the binding pocket of the protein has a preference for a hydrophobic substituent at the C7-position of tryptamine.

The pockets surrounding the ligand apparently have different electrostatic characteristics in the directions defined from the C5 and C7 positions of 5-HT; the milieu of the pocket near C7 seems to be mostly hydrophobic, whereas the milieu around C5 substituents seemingly is more hydrophilic (Figure 3). Note that the two binding modes from the IFD simulations exactly differ in their opposite orientations of C5 and C7 of 5-HT in the binding site. Thus, mutations of residues lining the ligand binding cavity along C5, C6, and C7 of the indole ring (Ala169, Ala173, and Thr439) were constructed to further discriminate the two binding modes employing the PaMLAC paradigm.

4.2.6. Ala169 and Substituted Tryptamines. Ala169 is predicted to be located near 5-HT C5 in IFD cluster 1 and near C6 and C7 in IFD cluster 2/3 but with the side chain pointing away from the substrate and probably not interacting directly with 5-HT. When Ala169 is mutated to the bulkier isoleucine, the affinities of the three C6-substituted tryptamines are virtually unaffected compared to wt hSERT. The affinity of Ala169Ile for tryptamine (7.6 μM) decreases 3-fold compared to wt hSERT (2.4 μM), indicative of an overall negative impact of this mutation on tryptamine binding. The same relative decrease is observed for 5-HT and 7-MeT in the Ala169Ile mutant compared to the wt, indicating that neither the apparent hydrophilicity of the pocket near C5 nor the hydrophobicity of the pocket near C7 is affected by this mutation. However, 5,7-diHT is significantly reduced in affinity by the Ala169Ile mutation relative to 5-HT, from 42 μM toward the wt to 520 μM against Ala169Ile. This could be interpreted as a repulsion between Ala169Ile and the hydroxyl substituent on C7 of the ligand and thus suggests that the Ala169 side chain and C7 of the ligand are close in space. Curiously, hydrophobic substituents on the C5 position (5-MeT, 5-MeOT) seem to have a positive effect on affinity when paired with Ala169Ile that could be interpreted as proximity of C5 of the ligand and Ala169. As noted above, the absence of a clear pattern in measured binding affinities of the Ala169Ile mutant may be due to secondary effects, which is consistent with structures predicted from IFD (Figure 2); the side chain of Ala169 is pointing away from the binding cavity, thus making a direct interaction less likely.

4.2.7. Ala173 and the 5-HT C5-Position. From the IFD clusters it can be speculated that mutants with long hydrophobic side chains at position 173 can potentially affect the affinity of substituted tryptamines in a manner that would allow us to deduce the correct location of the 5-HT C5 and C7 positions in the binding site. Accordingly, both leucine and methionine residues at position 173 have a negative impact on the affinity of tryptamine analogues with a hydrophilic substituent on C5 (5-HT) whereas the affinity of 7-MeT is unaffected. The affinity of 5,7-diHT is reduced 4−7 fold by the Ala173Met and Ala173Leu mutations which is actually less than the 7−18 fold reductions in affinity seen for 5-HT, indicating that the long hydrophobic side chains at position 173 do not interact negatively with a hydrophilic substituent on C7 but only with hydrophilic substituents on C5. In accordance, long hydrophobic residues on position 173 increase the affinity of tryptamine analogues with hydrophobic substituents on C5 (5-MeT and 5-MeOT) whereas it leaves 7-MeT and 7-MeOT affinities unaffected. All of these observations demonstrate that Ala173Met and Ala173Leu can transform the hydrophilic pocket near C5 to a hydrophobic one but will leave the hydrophobic pocket around C7 unaffected.

4.2.8. Thr439 and the 5-HT C5-Position. Mutagenesis of Thr439 to serine, alanine, and valine reveals a pattern in the affinity for C5-substituted tryptamines consistent with the side chain of Thr439 lining the hydrophilic pocket near C5. While tryptamine affinity is unchanged by Thr439Ala or Thr439Val mutations and slightly improved by the conservative mutation to serine, the affinity of tryptamines with hydrophobic substituents at the C5-position (5-MeT and 5-MeOT) benefit 14- to 22-fold by a Thr439Ala mutation. The Thr439Val mutants also exhibit improvements in affinity for tryptamines with hydrophobic substituents on C5 but to a lesser extent than seen for Thr439Ala. Furthermore, there is a trend toward reduced affinity of tryptamines with hydrophilic C5-substituents (5-HT and 5,7-diHT) for Thr439Val. This trend is even more pronounced for Thr439Ala. There is thus a clear indication that Thr439 mutations can influence the hydrophobicity of the pocket near C5 while leaving the pockets near C6 and C7 almost unaffected.

4.2.9. Mutation of Tyr175 and Tyr176. Mutation of the conserved Tyr175[25] to phenylalanine produces a mutant that has a dramatically decreased V_{max} (data not shown). An overall moderate increase in affinity for the tryptamines against Tyr175Phe is observed but otherwise no remarkable patterns can be detected. The completely conserved Tyr176 can be mutated to phenylalanine without significant changes in K_m or

V_{max} even though it forms a hydrogen bond to Asp98 in all theoretical models. No changes or patterns in the affinity of tryptamine analogues are seen for Tyr176 mutations. This may indicate that Tyr175 and Tyr176 are mostly important in substrate permeation and not particularly in the binding.

5. Discussion

5.1. Model of hSERT Structure and 5-HT Binding. It can be assumed that the substrate binding site of hSERT has the same approximate location as that of leucine in $LeuT_{Aa}$ since it would be highly improbable that a homologous transporter with similar ionic coupling should utilize a different binding site for the substrate.[9,12] A substrate binding site deep within the transporter, halfway through the membrane, is also consistent with predictions from studies employing a fluorescent NET substrate.[55]

The three employed sequence alignments of hSERT with $LeuT_{Aa}$ are highly similar, showing sequence identities of approximately 28% in the TM region. For membrane proteins this has been shown to produce homology models that will have RMSD values in the TM region of around 2 Å for Cα atoms compared to the native structure[31] when using a high-resolution template structure. Most importantly, the alignment of the helices making up the binding cavity, TM1, TM3, TM6, and TM8, surrounding the binding site are exactly identical in the three alignments, while differences are located in helices TM4, TM5, TM9, and TM12. Despite the high degree of similarity, though, alignment B resulted in homology models of hSERT, which are not suitable for placing 5-HT in the binding cavity, even when including protein flexibility during docking as in the IFD protocol. This points to the effects distant structural elements may have on the size and shape of the binding site and emphasizes the importance of a correct sequence alignment for the protein as a whole. Furthermore, it shows that choosing appropriate homology models with a large cavity is indeed important.

The unwound regions of TM1 and TM6 in the $LeuT_{Aa}$ structure are convincingly reproduced in the homology models (Figure 1). Figure 4 displays the two coordination environments for the sodium ions imported from the $LeuT_{Aa}$ structure (Figures 4A and 4B). Although the coordination around the ions is not perfect in the models, they are similar to the two sites in $LeuT_{Aa}$.[9,12] As predicted by Yamashita et al., Asp98 in hSERT substitutes for the coordination of Na1 to the carboxylate group from the substrate leucine in the $LeuT_{Aa}$ structure.[12] Residues Tyr121, Ser336, Asn368, and Ser372 are furthermore positioned so they can coordinate a chloride ion, forming a Cl^- binding site (Figure 4C) as has recently been shown.[24,30] In Figure 4D the substrate leucine from the template is depicted together with hSERT Asp98 and bound 5-HT. It is obvious that the oxygen atoms from the Asp98 carboxylate replaces those from the leucine carboxylate group. The same is seen for the 5-HT and leucine ammonium nitrogen atoms. In the three clusters identified from IFD the charged nitrogen of 5-HT is placed within 1 Å of the nitrogen atom from the superimposed leucine substrate from $LeuT_{Aa}$. This can be interpreted as an example of the *deletion model* as proposed for the evolution of selective receptors.[17]

(55) Schwartz, J. W.; Blakely, R. D.; DeFelice, L. J. *J. Biol. Chem.* **2003**, *278*, 9768−9777.

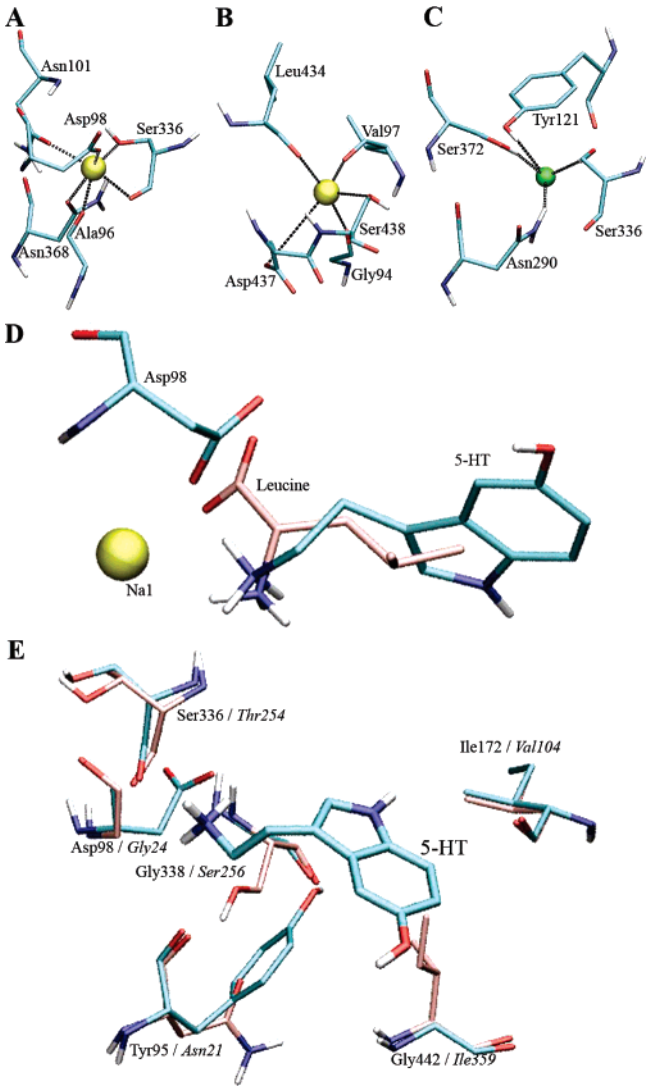

Figure 4. Coordination of (A) Na1, (B) Na2, and (C) Cl^- in hSERT models. (D) Asp98 and 5-HT bound in hSERT have similar functional groups as leucine in $LeuT_{Aa}$. (E) Differences in the hSERT···5-HT (cyan) and $LeuT_{Aa}$ (pink) binding sites. $LeuT_{Aa}$ residue numbers are given in italics. Based on cluster 3.

Only six out of 25 residues within 5 Å of 5-HT in hSERT differ from those in $LeuT_{Aa}$ (Figure 4E). A major difference is the mutation of $LeuT_{Aa}$ Gly24 to hSERT Asp98. This mutation is generally found between amino acid and monoamine transporters. Two other mutations are $LeuT_{Aa}$ Asn21 and Ser256 to hSERT Tyr95 and Gly338, respectively. These two residues form the protein surface that interacts with the aliphatic side chain of 5-HT. An extra aromatic residue was thereby introduced in hSERT and to allow for possible $\pi-\pi$ interactions between Tyr95 and 5-HT. It could be interesting to mutate this residue in hSERT and examine the need for an aromatic residue at the position of Tyr95 as well as the possibility of a larger residue instead of Gly338. The mutations of $LeuT_{Aa}$ Val104 and Thr254 to hSERT Ile172 and Ser336 are probably by themselves the least significant among the six differences; the methyl groups introduced or removed in hSERT do not face the binding site but the surrounding helices, thereby neither changing the size nor the electrostatics properties of the binding site. More important is the mutation of $LeuT_{Aa}$ Ile359 to hSERT Gly442. This residue is residing in the bottom of the cavity making up

the hydrophobic floor together with Ala169, Ile172, and Ala173 in the hSERT models. When superimposing the $LeuT_{Aa}$ and hSERT structures, it is seen, Figure 4E, that the position of the $LeuT_{Aa}$ Ile359 side chain coincides with that of the six-membered ring of the 5-HT indole ring. Altogether it can be suggested that the difference in substrate selectivity between $LeuT_{Aa}$ and hSERT may be found in the $LeuT_{Aa}$ to hSERT Ile359 to Gly442, Asn21 to Tyr95, and Gly24 to Asp98 mutations. A consequence of the mutations of Val104 and Ile359 in $LeuT_{Aa}$ to Ile172 and Gly442 in hSERT is that the hydrophobic pocket is opened and the two residues residing behind the hydrophobic contact of Val104 and Ile359 in $LeuT_{Aa}$ are exposed to the ligand in the hSERT binding cavity. These residues are Ala173 and Ala169. On the basis of the results for mutation of a creatine transporter into a GABA selective transporter,[18] one can envision that a few core mutations of hSERT may give a transporter that is, for example, selective for leucine.

The IFD simulations resulted in the identification of two possible binding orientations of 5-HT in the binding cavity. Both orientations show a salt bridge from Asp98 to the protonated amine of 5-HT, and the ligand was oriented to involve a contact between C6 of 5-HT and Ala173. The differences between the two binding modes are related to the orientation of the indole ring in the cavity; that is the interactions to C5, C7, and the indole N−H. Neither of the preliminary homology modeling studies[24−26,28,30] were able to place the ligand in the hSERT binding site by automated docking techniques nor could they provide any details regarding the orientation of 5-HT in the cavity. Thus, the binding mode identified in an MD simulation of 5-HT in hSERT,[56] where 5-HT was manually placed in a large cavity originally created by S-citalopram and introducing further restrained minimizations, differs from both of the binding modes detected from our more objective docking study. To the best of our knowledge, no other study in literature has considered the orientation of 5-HT in the cavity. The role of having a chloride ion present in the recently proposed Cl^--binding site was evaluated by a few additional IFD computations (listed in the Supporting Information). Briefly, it can be concluded that all homology models accommodate a chloride ion nicely. Furthermore, neither the statistics of the poses generated in IFD nor the computed docking scores change significantly depending on the presence of the anion. Thus, it seems likely that the role of the anion is related to transport and not directly involved in substrate binding.

5.2. Binding vs Transport of Tryptamines. Tryptamines can either be substrates,[57] i.e., they are transported, or inhibitors of hSERT. Thus, the measured K_i may reflect affinities toward other conformational states of the transport cycle. Apart from the natural substrate 5-HT, the most potent substrate for wt hSERT in this study is 5,7-diHT. It is transported with only 12% of the efficiency of 5-HT[57] but also exhibits a 46-fold lower K_i than 5-HT (see Table 3), easily accounting for the reduced transport. Comparison of the binding affinities (by K_i values) with the results for transport measured by Pratuangdejkul et al.[57] reveals a poor correlation between transport efficiency and binding affinity for tryptamines in hSERT, unless a hydroxy or methoxy substituent is present at the C5-position. Binding of a tryptamine is thus a prerequisite for transport but not sufficient to trigger it. Accordingly, 5-HT, 5,7-diHT, 6-HT, and 5-MeOT were transported with efficiencies mirroring their relative affinities whereas tryptamine, 5-MeT, 2C, 6-MeOT, and 6-FT were transported poorer (or not at all) than expected from their inhibitory potencies. The observation that 6-HT can be transported indicates some promiscuity in hSERT and could be a result of structural flexibility of either substrate or protein, however, not extending this to a methoxy group at the C6-position, 6-MeOT. A study detailing the kinetic properties of a fluorescent substrate for hNET, showing that binding and unbinding of the substrate will occur 36 000 times for each transport event,[58] supports the notion that binding and triggering of translocation are two separate events. The rate-limiting translocation is not initiated by binding *per se* but can be speculated to be so by the presence of a hydrophilic (oxygen) substituent on C5 of the tryptamine. Since both IFD cluster 2/3 and the mutational studies suggest a possible interaction between 5-HT and Thr439 located in TM8 next to Ser438, which interacts with Na2, one can speculate that simultaneous presence of substrate and Na2 might induce the formation of the observed kinks in TM8. It is known that TM8 undergoes conformational changes as part of the transport process,[59] and it can be hypothesized that this serves as the communication link between favorable binding events in the binding site and the formation of an intracellular permeation pore.[60,61]

5.3. Salt Bridge between Asp98 and 5-HT. Within the monoamine transporter subfamily of NSSs, Asp98 is fully conserved. Other members of the NSS family, the amino acid transporters, predominantly have a glycine at this position. The inference that the acidic side chain forms a salt bridge with the protonated primary amine of the cognate substrate of SERT, DAT, and NET was originally reported by Kitayama et al.[62] but later questioned by Wang et al.[63] In hSERT the findings of Barker et al.[19] and the present study show that the loss of affinity when shortening the alkylamine chain of tryptamine can be partially rescued by lengthening the acidic side chain at position 98 of hSERT. The inability to fully rescue the affinity of 1A in Asp98Glu can be rationalized by the fact that 1A has a reduced flexibility due to the short alkyl chain, when adapting to the interaction with an acidic residue at position 98.

5.4. Enantioface Discrimination of the Indole Moiety. The 5-HT indole ring constitutes a prochiral fragment and the two binding modes identified from IFD can be regarded as the recognition of the two enantiofaces. The main difference is the interchanging positions of C5 and C7 as well as the direction of the indole N−H bond. The enantioface discrimination of the two 5-HT binding modes might thus be due to interactions from the indole N−H to the binding site. It has been suggested that

(56) Jørgensen, A. M.; Tagmose, L.; Jørgensen, A. M. M.; Bøgesø, K. P.; Peters, G. H. *ChemMedChem* **2007**, *2*, 827−840.
(57) Pratuangdejkul, J.; Schneidier, B.; Jaudon, P.; Rosilio, V.; Baudoin, E.; Loric, S.; Conti, M.; Launay, J. M.; Manivet, P. *Curr. Med. Chem.* **2005**, *12*, 2393−2410.
(58) Schwartz, J. W.; Novarino, G.; Piston, D. W.; DeFelice, L. J. *J. Biol. Chem.* **2005**, *280*, 19177−19184.
(59) Norregaard, L.; Loland, C. J.; Gether, U. *J. Biol. Chem.* **2003**, *278*, 30587−30596.
(60) Loland, C. J.; Norregaard, L.; Litman, T.; Gether, U. *Proc. Natl. Acad. Sci. U.S.A.* **2002**, *99*, 1683−1688.
(61) Guptaroy, B.; Zhang, M.; Binda, F.; Bowton, E.; Johnson, L.; Galli, A.; Javitch, J.; Gnegy, M. *Society for Neuroscience Annual Meeting*, Atlanta, GA, U.S.A., October 14−18, 2006 and personal communication.
(62) Kitayama, S.; Shimada, S.; Xu, H.; Markham, L.; Donovan, D. M.; Uhl, G. R. *Proc. Natl. Acad. Sci. U.S.A.* **1992**, *89*, 7782−7785.
(63) Wang, W.; Sonders, M. S.; Ukairo, O. T.; Scott, H.; Kloetzel, M. K.; Surratt, C. K. *Mol. Pharmacol.* **2003**, *64*, 430−439.

Phe341 in hSERT is involved in $\pi-\pi$ stacking with 5-HT.[12] Indeed, according to the models, Phe341 receives π-stabilization by interacting with the indole N−H in an orthogonal "T-shape"-manner in clusters 2 and 3 from IFD. This has been shown to be as favorable as the parallel-displaced $\pi-\pi$ stacking conformation for benzene rings.[64,65] In cluster 1 an orthogonal T-shaped interaction of indole N−H is found with Tyr176 located at the opposite face of the binding cavity. Similar hydrogen bonds to π-systems have previously been shown to be important in proteins for stabilizing the local 3D structure.[66] Mutations of these two aromatic residues to non-aromatic ones may accordingly be able to shed further light on this interaction, assuming that the transporter remains active.

In IFD clusters 2 and 3, which were shown above to be consistent with the data from the PaMLAC studies, the hydrophilic pocket around C5 is predicted to be formed at the interface of TM3 and TM8, and more precisely by the side chains of residues Ala173 and Thr439. As shown above, results from mutations of these two residues and binding of tryptamine analogues substituted at C5, C6, or C7 are consistent with the predictions formed on the basis of IFD clusters 2 and 3 while inconsistent with predictions from IFD cluster 1.

6. Conclusion

In conclusion we have provided evidence from computations, SAR, and mutagenesis studies under the PaMLAC paradigm that (a) hSERT Asp98 interacts with the protonated alkylamine of 5-HT, (b) hSERT Ala173 mutants interact with tryptamines substituted at the C6 position (Figure 2D), (c) the electrostatic properties of hSERT changes from a hydrophilic vicinity of the 5-HT C5-position to a hydrophobic area around the 5-HT C7-position (Figure 3), (d) long hydrophobic side chains on hSERT residue 173 can extend into the pocket near the 5-HT C5-position, and (e) hSERT Thr439 interacts with the hydroxyl group of 5-HT. These observations are only consistent with a 5-HT binding mode in hSERT as found in clusters 2 and 3 in the IFD calculations. We expect that this model will be of great importance for understanding the function of hSERT and for future drug design projects. Current research in our group is aimed at describing the movements of the cytoplasmic parts of TM1, TM6, and TM8 relative to one another, which would be useful in taking the understanding of hSERT function one step further. Studies to further elucidate the monoamine transporters as drug targets are similarly underway.

Acknowledgment. We thank Bente Ladegaard for skilful technical assistance and the iNANO Center, the Danish Center for Scientific Computing, the Danish Natural Science Research Council, the Danish National Research Foundation, and the Carlsberg and Lundbeck Foundations for financial support.

Note Added after ASAP Publication: The version of this paper published on March 4, 2008, contained errors involving refs 14 and 24. The version published on March 6, 2008 has the correct information.

Supporting Information Available: Details of the experimental methods; figures of computed DOPE per residue scores and the alignments against $LeuT_{Aa}$; a table with GlideScore, IFDScore, and hydrogen bond distances for Asp98···5-HT; results from simulations with Cl^- included in the models. This material is available free of charge via the Internet at http://pubs.acs.org. A pdb file with 5-HT bound in hSERT can be obtained from the authors.

JA076403H

(64) Sinnokrot, M. O.; Valeev, E. F.; Sherrill, C. D. *J. Am. Chem. Soc.* **2002**, *124*, 10887−10893.
(65) Sinnokrot, M. O.; Sherrill, C. D. *J. Phys. Chem. A* **2004**, *108*, 10200−10207.
(66) Steiner, T.; Koellner, G. *J. Mol. Biol.* **2001**, *305*, 535−557.